Incorporation of quantum dots on virus in polycationic solution

Jin-Oh You[1]
Yu-San Liu[2]
Yu-Chuan Liu[1]
Kye-Il Joo[1]
Ching-An Peng[1,2]

[1]Department of Chemical Engineering and [2]Department of Materials Science, University of Southern California, Los Angeles, CA, USA

Abstract: Developing methods to label viruses with fluorescent moieties has its merits in elucidating viral infection mechanisms and exploring novel antiviral therapeutics. Fluorescent quantum dots (QDs), an emerging probe for biological imaging and medical diagnostics, were employed in this study to tag retrovirus encoding enhanced green fluorescent protein (EGFP) genes. Electrostatic repulsion forces generated from both negatively charged retrovirus and QDs were neutralized by cationic Polybrene®, forming colloidal complexes of QDs–virus. By examining the level of EGFP expression in 3T3 fibroblast cells treated with QDs-tagged retroviruses for 24 hours, the infectivity of retrovirus incorporated with QDs was shown to be only slightly decreased. Moreover, the imaging of QDs can be detected in the cellular milieu. In summary, the mild method developed here makes QDs-tagged virus a potential imaging probe for direct tracking the infection process and monitoring distribution of viral particles in infected cells.

Keywords: endocytosis, infection, envelope protein, Polybrene®, quantum dots, retroviral transduction

Introduction

The endocytic pathways of viral infection have been studied to elucidate the underlying mechanisms and exploit potential therapeutic strategies to prevent virus-triggered diseases (Sieczkarski and Whittaker 2002; Lakadamyali et al 2004). Electron microscopy, which can clearly show the morphology of viral nanoparticles, has been used to study virus–cell interactions of HIV (Pudney and Song 1994). Confocal laser scanning microscopy has been used for visualization of immunostained retroviral particles (Pizzato et al 1999). However, both electron microscopy and confocal analysis of immunostained particles do not allow monitoring of the dynamic process of viral infection let alone intracellular trafficking. Indeed, many critical features of entry mechanisms and endocytic trafficking of virus still remain unclear (Friedman 1997; Pelkmans and Helenius 2003; Rust et al 2004). To unravel viral endocytic mechanisms by tracking a single viral particle in real-time imaging, fluorescent dye has been recently used widely for viral labeling experiments, and has improved our understanding of the viral infection process (Georgi et al 1990; Seisenberger et al 2001; Nunes-Correia et al 2002; Lakadamyali et al 2003). However, fluorophores are notorious for photobleaching and spectral overlaps, and therefore could affect the efficacy of tracking dye-labeled virus. In view of the drawbacks of using fluorescent dyes (Chan and Nie 1998; Parak et al 2005), colloidal semiconductor quantum dots (QDs) were investigated in this study to explore the potency of tagging QDs to viral particles. Thanks to excellent photostability, broad adsorption spectra, and narrow emission spectra, QDs have attracted great interest in many areas of research from molecular and cellular biology to molecular imaging and medical diagnostics (Michalet et al 2005 and references therein).

Correspondence: Jin-Oh You
Department of Chemical Engineering, University of Southern California, 925 Bloom Walk, HED 208, Los Angeles, CA 90089-1211, USA
Tel + 1 213 740 2067
Fax + 1 213 740 8053
Email jyou@usc.edu

To construct a QDs–virus imaging modality capable of providing meaningful information, preservation of viral infectivity after tagging virus with QDs is of utmost importance. As a first step towards functional QDs–virus imaging probes, Moloney murine leukemia retrovirus (MoMLV)-based retroviral vector encoding enhanced green fluorescent protein (EGFP) was selected as the biological model system to interact with inorganic QDs. Retroviral vector is the most commonly used system in gene therapy trials due to its ability to permanently integrate a therapeutic transgene into a target cell chromosome (Mountain 2000). The envelope proteins on the retrovirus surface play a pivotal role in cell membrane fusion, viral entry via endocytosis, and endosomal escape of viral particles (Frederickson and Whitt 1995; McTaggart and Al-Rubeai 2002). Since retroviral particles have a short a half-life of 5–8 hours at 37 °C due to shedding of envelope proteins from the viral surface (Kwon et al 2003), the physical–chemical process involved in incorporating retrovirus with QDs needs to be mild. Otherwise, retroviral infectivity could be diminished even though QDs are tagged on the viral surface.

Complexes between QDs and retrovirus, both possessing a net negative surface charge, were formed by colloidal clustering, facilitated by positively charged Polybrene® (hexadimethrine bromide) in the solution. Polybrene is a cationic polymer and has been reported to act by neutralizing negative charges on the surface of cells and virions to promote virus attachment and enhance viral transduction rate (Kwon and Peng 2002; Davis et al 2004). Retroviruses tagged with QDs were used to infect NIH 3T3 fibroblast cells to examine if retroviral infectivity is preserved and imaging of QDs can be detected intracellularly.

Materials and methods

Synthesis of CdSe–ZnS quantum dots

To prepare semiconductor CdSe–ZnS nanocrystals, methods reported previously were adopted with a slight modification (Reiss et al 2002; Huang et al 2004). All reagents were used as purchased from Sigma-Aldrich (St Louis, MO, USA) without further purification. A mixture of 25.68 mg of CdO, 3.88 g of tri-n-octylphosphine oxide (TOPO), and 2.41 g of hexadecylamine (HDA) was heated to 320 °C under a dry nitrogen atmosphere. After the formation of a CdO–HDA complex as indicated by the change of color from reddish to colorless, the temperature of the solution was cooled to 300 °C. A stock solution with 31.58 mg of Se dissolved in 5 mL of tributylphosphine (TBP) was quickly injected into the solution under rigorous stirring to nucleate CdSe nanocrystals. After injection, the core solution was grown at 300 °C for ~5 seconds when the color of the mixture turned from colorless to slightly red. The temperature was then cooled to 220 °C for shell growth. The shell solution containing zinc stearate (379.4 mg) and sulfur powder (12.8 mg) dissolved in TBP (5 mL) was heated to 110 °C for 30 minutes and then cooled to room temperature for injection. The shell solution was added dropwise into the core solution under thorough stirring over a period of 15 minutes. After the addition of shell solution, the core–shell solution was cooled down to 120 °C to anneal for 2 hours. The core–shell solution was cooled to room temperature afterwards. The CdSe–ZnS nanocrystals were precipitated by anhydrous methanol and then stored in anhydrous toluene for further use.

Solvation of CdSe–ZnS QDs

To make QDs water soluble for biological use, a ligand exchange method using mercaptoacetic acid (MAA) was performed (Chan and Nie 1998). The colloidal QDs were dissolved in chloroform and reacted with glacial MAA (~1 M) for 2 hours. An aqueous phosphate buffered saline (PBS) solution (pH 7.4) was added to this reaction mixture at a 1:1 volume ratio. After vigorous mixing, the chloroform and water phase separated spontaneously. The aqueous phase containing MAA-capped QDs was extracted. MAA-capped QDs were collected by centrifugation at 14 000 rpm for 10 minutes (Eppendorf microcentrifuge Model 5415C, Brinkman Instruments Inc, Westbury, NY, USA).

Photoluminescence spectrum

The photoluminescence (PL) spectrum of QDs was measured by a fluorometer (SpectraMax M2, Molecular Devices Corp, Sunnyvale, CA, USA) with an excitation wavelength of 480 nm. The scanning step was set as 1 nm.

Particle size analysis

MAA-capped QDs were dispersed in aqueous solution by a sonicator (550 W, 20 kHz; Misonix, Farmingdale, NY, USA) for 3 minutes and then run through reversed phase silica gel 100 C_{18} (Sigma-Aldrich, particle size 15–35 μm) in a chromatography column (Sigma-Aldrich, 460 × 10 mm) to collect nonaggregated QDs. MAA-capped QDs were analyzed for mean particle size and size distribution by the dynamic light scattering DynaPro-99EMS/X (Wyatt Technology Corp, Santa Barbara, CA, USA) equipped with

a diode-pumped solid-state laser operating at 655 nm wavelength as a light source at 25 °C, controlled with Micro-Sampler temperature controller. The particle size distribution and the average particle diameter were obtained from the correlation function by a regularization method included in the data analysis software package (Dynamics V6.3.01).

Retroviral production

$GP^{+}E86$ packaging cells encoding EGFP genes were cultured in Dulbecco's modified Eagle's medium (DMEM) supplemented with 10% fetal bovine serum (FBS; Gibco BRL, Rockville, MD, USA). When cell confluence reached 80%, culture media were taken out and rinsed 3 times with PBS. The packaging cells were further cultured in fresh DMEM with 10% FBS (designated as D10 medium). Every 24 hours, EGFP-containing retroviral supernatants were collected and replaced with fresh culture medium. The collected culture medium (up to 72 hours) was filtered through a 0.45 μm filter and stored at −80 °C for later use.

Transduction of NIH 3T3 cells by QDs-tagged retrovirus

MAA-capped QDs suspended in 1 mL D10 medium were added into 1 mL retrovirus-containing medium. After gentle shaking of the mixed media, Polybrene (Sigma-Aldrich) stock solution was pipetted into the mixture to give a final concentration of Polybrene of 8 μg/mL. Then, the mixed solution was incubated at 4 °C for 1 hour to prevent retroviruses from losing activity. After the process of tagging QDs to retrovirus had been performed for 1 hour, 5×10^4 NIH 3T3 cells in exponential growth phase were replaced with the pre-incubated QDs–retrovirus-containing medium. Twenty-four hours after addition of QDs-tagged retrovirus, transduction rate was determined by counting cells expressing EGFP protein in 5 fluorescent confocal microscopic fields. After the culture well was gently washed by PBS to remove QDs in the extracellular medium, the intracellular locations of QDs were detected by fluorescent confocal microscopy (Zeiss LSM 510 META, Carl Zeiss Inc, Thornwood, NY, USA). As a control group, cells were infected with retrovirus without QDs tagging under the same conditions as above.

Results and discussion

Characterization of QDs

Since MAA-capped QDs are not very stable in water (Willard et al 2001) and could form agglomerates, QDs-containing aqueous solution was run through a silica gel column to collect well-dispersed QDs. The dynamic light scattering data obtained for these collected QDs had an average size of 27.7 nm (Figure 1). Recent work suggested that the hydrodynamic diameters of QDs could be considerably larger than their transmission electron

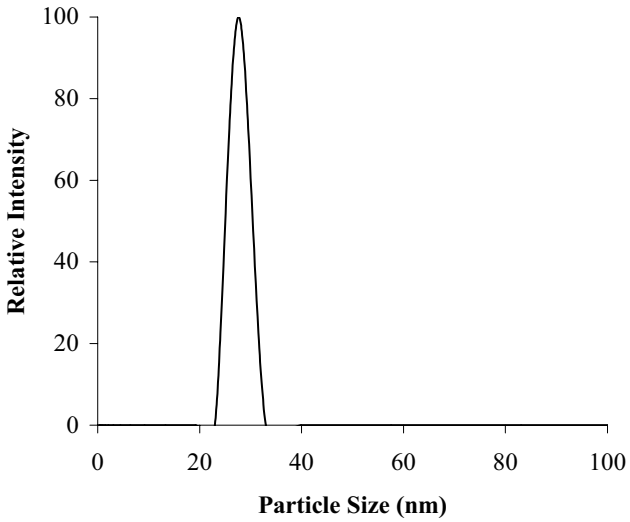

Figure 1 Dynamic light scattering size-distribution profile for mercaptoacetic acid (MAA)-capped quantum dots (QDs). After sonicator treatment and silica gel separation, particle size distribution was narrowed down to the range between 20 and 35 nm. The mean particle diameter was 27.7 nm.

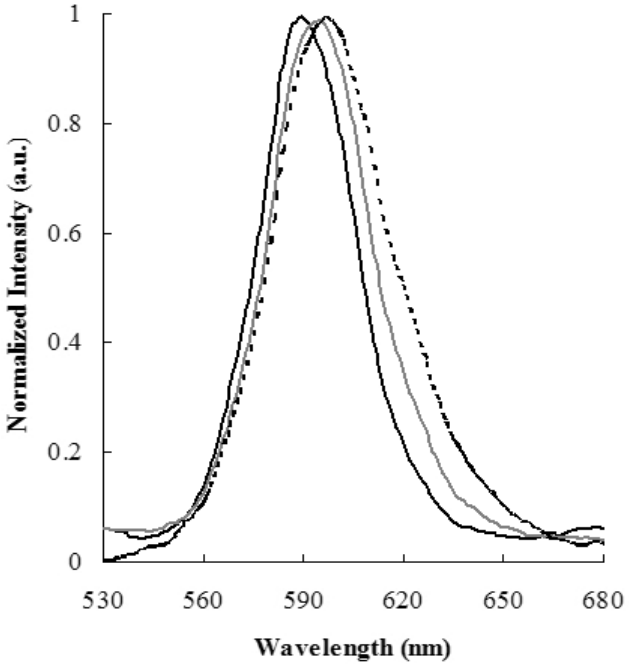

Figure 2 Emission spectra of CdSe–ZnS. The emission spectra of tri-n-octylphosphine oxide (TOPO)-capped CdSe–ZnS in toluene and mercaptoacetic acid (MAA)-capped CdSe–ZnS in de-ionized water are shown as dashed and solid lines, respectively. The gray line represents the emission spectrum of MAA-capped quantum dots (QDs) associated with retroviruses in Polybrene-containing solution.

microscope (TEM) "dry" diameters, since organic materials are not electrondense enough for TEM visualization on the nanometer scale (Larson et al 2003). Figure 2 shows the photoluminescence spectra of QDs capped with TOPO, MAA, and tagged with retrovirus, respectively. The dashed line represents the spectrum of QDs capped by TOPO suspended in toluene with the emission wavelength peaked at 601 nm. The solid line represents the spectrum of MAA-capped QDs suspended in deionized water, revealing the emission wavelength peaked at 593 nm. Such a miniscule blue shift of the spectrum detected on MAA-capped QDs was probably caused by the change of surface ligands from TOPO to MAA (Hanaki et al 2003). The gray line shows MAA-capped QDs associated with retroviruses by Polybrene, and the emission wavelength peak shift to 598 nm. The red shift is probably because MAA-capped QDs interact with Polybrene by electrostatic absorption. The quantum yield (QY) was calculated to be 12.2% and 0.19% before and after water-solubilizing with MAA, respectively, and 1.1% after tagging with viruses, by comparing the photoluminescence intensity of QDs with that of rhodamine 6G (QY = 95%). After phase transfer to aqueous, the fluorescent intensity of QDs dropped and then recovered slightly after tagging with retroviruses. Polybrene probably neutralized the surface charge of MAA-capped QDs and altered the environment polarity of MAA-capped QDs.

Efficient QDs-tagged retrovirus

Figure 3 shows the photomicrographical images of NIH 3T3 cells as the control groups in this study. If QDs were added into the cell culture dish in the absence of Polybrene, MAA-capped QDs were not detected under the fluorescent confocal microscope after the cell layer was washed with PBS (Figure 3a). A few MAA-capped QDs were detected around the cell membrane if QDs were added in the presence of Polybrene (Figure 3a). In principle, extracellular QDs should be washed off by PBS prior to confocal microscopic observation. They were not washed off probably because the electrostatic neutralization effect of Polybrene led to nonspecific adsorption of negatively charged MAA-capped QDs on negatively charged cell membranes. It is clearly shown that QDs did not enter the intracellular domain. This observation is consistent with the data reported previously that MAA-capped QDs without binding transferrin were not transported through cell membranes (Chan and Nie 1998). However, after binding with transferrin, receptor-mediated endocytosis occurred and QDs could be viewed in the intracellular space. Figure 3c shows the NIH 3T3 cell expressing EGFP after 24 hours of retroviral transduction. The calculated percentage of EGFP-expressing cells (ie, retroviral transduction rate) was 78%. The question is whether the QDs-tagged retroviruses are able to interact efficiently with retroviral receptors on 3T3 cells and attain the level of EGFP expression given in Figure 3c.

The envelope proteins deployed on the surface of retrovirus are indispensable for receptor-mediated endocytosis. The key proteins of the infection process are the retroviral surface protein (SU) and transmembrane protein (TM). SU is located extracellularly and linked to TM by non-covalent interaction. Because of the weak association of SU and TM, SU is easily shed from the surface of viral particles (eg, 50% loss of retroviral infectivity within 5–8 hours at 37 °C). Therefore, it is a challenge to retain retroviral infectivity after tagging retroviruses with QDs.

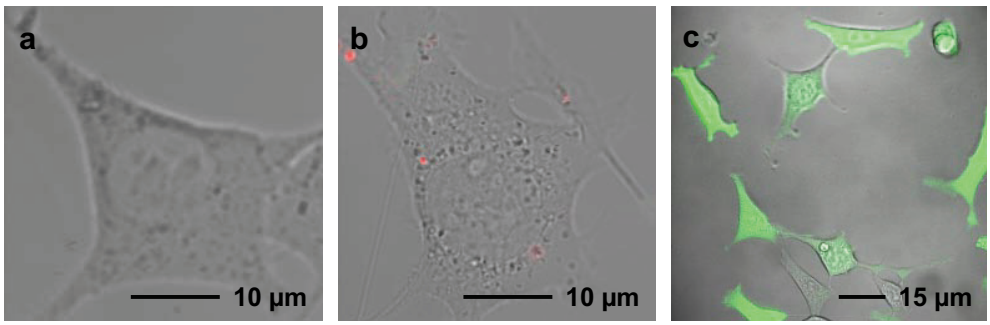

Figure 3 Photomicrographical images of NIH 3T3 cells exposed separately to quantum dots (QDs) and retrovirus in the culture medium with and without 8 μg/mL Polybrene. (a) image of 3T3 cells incubated with QDs in the absence of Polybrene. QDs were not detected by fluorescent confocal microscopy after washing with phosphate buffered saline (PBS) 3 times. (b) image of 3T3 cells incubated with QDs in the presence of Polybrene. A few red dots indicate QDs were located around the cell membranes. QDs were not internalized into cell cytoplasm. However, they were attached to cell membrane due to the presence of positively charged Polybrene. (c) 3T3 cells exhibited enhanced green fluorescent protein (EGFP) expression after infection by retroviruses only. Percentage of EGFP-expressing cells counted under 5 fluorescent microscopic fields was 78%.

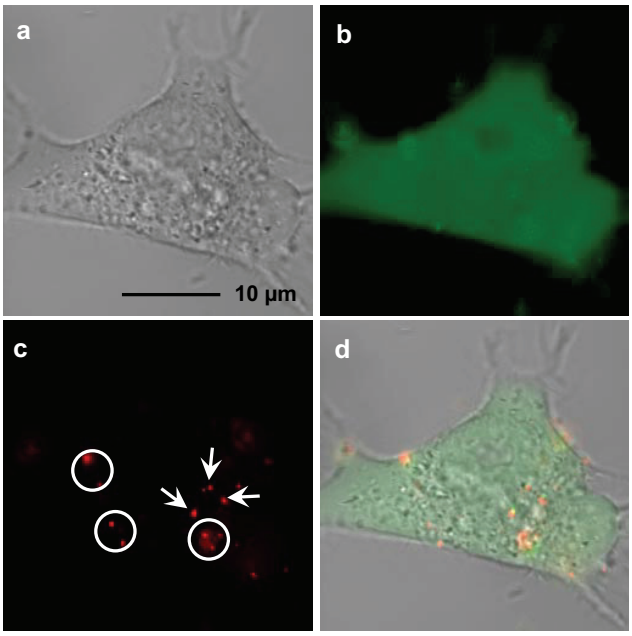

Figure 4 Photomicrographical images of NIH 3T3 cells treated with quantum dots (QDs)-tagged retroviruses. (a) and (b) were images taken under bright-field and fluorescent microscopy, respectively, after 24 hours of retroviral transduction. In (c), white circles indicate that QDs along with virus were endocytosed into cellular domain and white arrows indicate that a few QDs even entered the cell nucleus. (d) shows a combined image of (a) and (b). Yellowish color revealed colocalization of internalized QDs and expressed enhanced green fluorescent protein (EGFP) protein.

We have tried to covalently bind retroviruses with QDs using a water-soluble carbodiimide (eg, EDC). However, the retroviral transduction efficiency was very low (data not shown). It is speculated that the envelope proteins were shed from the retroviral surface under harsh covalent binding conditions. Therefore, the labeling process involved in incorporating retrovirus with QDs needs to be mild. Figure 4b reveals the image of EGFP expression of 3T3 cells transduced by retrovirus tagged with QDs using Polybrene. The calculated percentage of EGFP-expressing cells was 70%. Apparently, the mild tagging method decreased infectivity only slightly. As shown in Figure 4c, quite a few QDs were detected within the cell, indicating QDs were incorporated well onto the viral surface and ferried through cell portals via retrovirus-mediated endocytosis. Even small amounts of QDs, indicated by arrows, were observed in the cell nucleus. It is expected that other types of QDs capped by negatively charged water-soluble ligands (eg, dihydrolipoic acid) could also tag virus by the method described here. Furthermore, using QDs capped by positively charged water-soluble ligands to tag retrovirus without the aid of Polybrene is probably a feasible and simple method.

Conclusion

We have demonstrated the feasibility of tagging negatively charged retrovirus with carboxylate-terminated QDs at 4 °C via polycationic Polybrene. This mild methodology developed here could make QDs-tagged virus a functional imaging probe for the analysis of intracellular trafficking and cytoskeleton reorganization during virus entry.

Acknowledgments

This work was supported in part by grant R21 EB04117 from the National Institutes of Health.

References

Chan WCW, Nie SM. 1998. Quantum dot bioconjugates for ultrasensitive nonisotopic detection. *Science*, 281:2016–18.

Davis HE, Rosinski M, Morgan JR, et al. 2004. Charged polymers modulate retrovirus transduction via membrane charge neutralization and virus aggregation. *Biophys J*, 86:1234–42.

Frederickson BL, Whitt MA. 1995. Vesicular stomatitis virus glycoprotein mutations that affect membrane fusion activity and abolish virus infectivity. *J Virol*, 69:1435–43.

Friedman T. 1997. Overcoming the obstacles to gene therapy. *Sci Am*, 276:96–101.

Georgi A, Mottola-Hartshorn C, Warner A, et al. 1990. Detection of individual fluorescently labeled reovirions in living cells. *Proc Natl Acad Sci U S A*, 87:6579–83.

Hanaki KI, Momo A, Oku T, et al. 2003. Semiconductor quantum dot/albumin complex is a long-life and highly photostable endosome marker. *Biochem Biophys Res Commun*, 302:496–501.

Huang GW, Chen CY, Wu KC, et al. 2004. One-pot synthesis and characterization of high-quality CdSe/ZnX (X=S, Se) nanocrystals via the CdO precursor. *J Cryst Growth*, 265:250–9.

Kwon YJ, Hung G, Anderson WF, et al. 2003. Determination of infectious retroviral concentration from colony-forming assay with quantitative analysis. *J Virol*, 77:5712–20.

Kwon YJ, Peng CA. 2002. Transduction rate constant as more reliable index quantifying efficiency of retroviral gene delivery. *Biotechnol Bioeng*, 77:668–77.

Lakadamyali M, Rust MJ, Babcock HP, et al. 2003. Visualizing infection of individual influenza viruses. *Proc Natl Acad Sci U S A*, 100:9280–5.

Lakadamyali M, Rust MJ, Zhuang X. 2004. Endocytosis of influenza viruses. *Microbes Infect*, 6:929–36.

Larson DR, Zipfel WR, Williams RM, et al. 2003. Water-soluble quantum dots for multiphoton fluorescence imaging in vivo. *Science*, 300:1434–6.

McTaggart S, Al-Rubeai M. 2002. Retroviral vectors for human gene delivery. *Biotechnol Adv*, 20:1–31.

Michalet X, Pinaud FF, Bentolila LA, et al. 2005. Quantum dots for live cells, in vivo imaging and diagnostics. *Science*, 307:538–44.

Mountain A. 2000. Gene therapy: the first decade. *Trends Biotechnol*, 18:119–28.

Nunes-Correia I, Eulalio A, Nir S, et al. 2002. Fluorescent probes for monitoring virus fusion kinetics: comparative evaluation of reliability. *Biochim Biophys Acta*, 1561:65–75.

Parak WJ, Pellegrino T, Plank C. 2005. Labelling of cells with quantum dots. *Nanotechnology*, 16:R9–25.

Pelkmans L, Helenius A. 2003. Insider information: what viruses tell us about endocytosis. *Curr Opin Cell Biol*, 15:414–22.

Pizzato M, Marlow SA, Blair ED, et al. 1999. Initial binding of murine leukemia virus particles to cells does not require specific Env-receptor interaction. *J Virol*, 73:8599–611.

Pudney J, Song MJ. 1994. Electron microscopic analysis of HIV-host cell interactions. *Tissue Cell*, 26:539–50.

Reiss P, Bleuse J, Pron A. 2002. Highly luminescent CdSe/ZnSe core/shell nanocrystals of low size dispersion. *Nano Lett*, 2:781–4.

Rust MJ, Lakadamyali M, Zhang F, et al. 2004. Assembly of endocytic machinery around individual influenza viruses during viral entry. *Nat Struct Mol Biol*, 11:567–73.

Seisenberger G, Ried MU, Endreb T, et al. 2001. Real-time single-molecule imaging of the infection pathway of an adeno-associated virus. *Science*, 294:1929–32.

Sieczkarski SB, Whittaker GR. 2002. Dissection virus entry via endocitosis. *J Gen Virol*, 83:1535–45.

Willard D, Carillo L, Jung J, et al. 2001. CdSe-ZnS quantum dots as resonance energy transfer donors in model protein-protein binding assay. *Nano Lett*, 1:469–74.